Volume 64, Issue 5, May 2013   ISSN 0047-2484

Journal of Human Evolution

The artiodactyl calcaneus as a potential 'control bone' cautions against simple interpretations of trabecular bone adaptation in the anthropoid femoral neck

Kristofer D. Sinclair [a,b], Ryan W. Farnsworth [a,b], Theresa X. Pham [a,b], Alex N. Knight [a], Roy D. Bloebaum [a,b], John G. Skedros [a,b,*,1]

[a] Bone and Joint Research Laboratory, Department of Veterans Affairs Salt Lake City, Health Care System, 500 Foothill Boulevard, Salt Lake City, UT 84148, USA
[b] University of Utah School of Medicine, Department of Orthopedics, 590 Wakara Way, Salt Lake City, UT 84108, USA

ARTICLE INFO

ABSTRACT

For over a century, the arched trabecular patterns of the human proximal femur have been considered to resemble tension and compression stress trajectories produced by stereotypical bending loads. This reflects conventional modeling of the human femoral neck–head region as a short cantilevered beam. Although this conception is the foundation of many biomechanical, clinical, paleontological, and comparative morphological studies of trabecular bone in various species, attempts have not been made to contrast these data to a bone that could be considered a 'control' for simple/stereotypical bending. We quantified trabecular architectural characteristics in sheep and deer calcanei as a first step in potentially establishing them as 'controls' in this context because they have arched trabecular patterns that resemble tension/compression stress trajectories, and have been shown by strain gauge measurements to be relatively simply loaded in bending. Using micro-computed tomography, calcanei from adult domesticated sheep and wild deer were analyzed where in the dorsal 'compression' and plantar 'tension' trabecular tracts they begin to separate and bending is less complex (mid-shaft), and where trabeculae extensively interconnect and loading is more complex (distal shaft). Of the eight trabecular architectural characteristics evaluated, only one (trabecular number, Tb.N) showed a probable mechanically relevant dorsal/plantar difference. However, this was paradoxically opposite in the sheep calcanei. Aside from Tb.N, the architectural characteristics showed little, if any, evidence of habitual bending. The non-uniformity of the stresses between the trabecular tracts in these bones might be reduced by load-sharing functions of their robust cortices and the nearby ligament and tendon, which might account for the similar morphologies between the tracts. These findings may help to explain why in many cases regional trabecular architectural variations seem to lack sufficient sensitivity and specificity for interpreting habitual bending in other bone regions. This cautions against simple interpretations of trabecular bone adaptation in the anthropoid femoral neck.

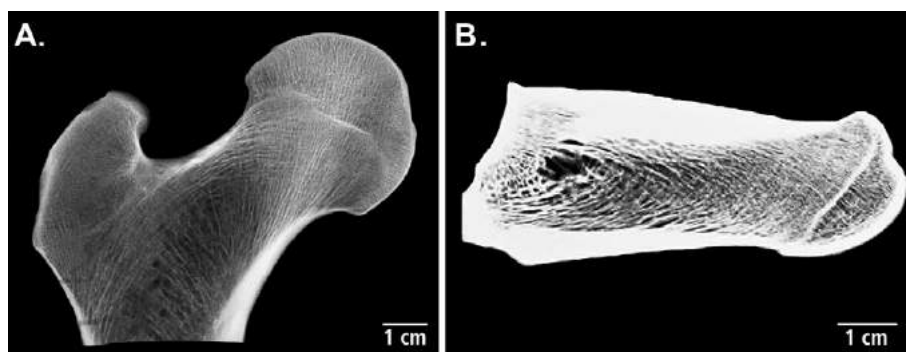Published by Elsevier Ltd.

Introduction

Femoral neck fractures can result in severe impairment of mobility and lifestyle, and in the elderly they are also associated with a mortality rate that can exceed 20% within two years of fracture (Boonen et al., 2004; Adachi et al., 2010; Ma et al., 2011). This has led to extensive studies of the biomechanics, structure, and histomorphology of the femoral neck in an attempt to understand the intrinsic factors that predispose individuals to fractures in this region. The natural history of this malady has also been considered in the context of developmental and evolutionary modifications of hip functional morphology associated with different degrees and types of physical usage and locomotor behaviors, the emergence of bipedalism, and the longevity of some modern populations (Lovejoy, 1988, 2004; Lovejoy et al., 2003; Mayhew et al., 2005; Fajardo et al., 2007; Kaptoge et al., 2007; Poole et al., 2010; Ryan and Walker, 2010; Shaw and Ryan, 2012). These studies have also advanced our understanding of the development and functional roles of cortical and trabecular (cancellous) bone mass, architecture, and histomorphology during normal loading of the femoral neck and how aging can change these relationships and ultimately

* Corresponding author.
  E-mail addresses: kristofer.sinclair@hsc.utah.edu (K.D. Sinclair), rfarnsw826@gmail.com (R.W. Farnsworth), txp@comcast.net (T.X. Pham), alexknight9@hotmail.com (A.N. Knight), roy.bloebaum@hsc.utah.edu (R.D. Bloebaum), jskedrosmd@uosmd.com (J.G. Skedros).
  [1] 5323 South Woodrow Street, Suite 200, Salt Lake City, UT 84107, USA.

Figure 1. (A) Anterior-to-posterior radiograph of a thin-sectioned (∼3 mm) human proximal femur. The section was made with the bone in internal rotation in order to orient the proximal femur in neutral (0°) anteversion (Skedros and Baucom, 2007). (B) Lateral-to-medial radiograph of a thin-sectioned (∼2 mm) right calcaneus from an adult mule deer. Sectioning removed the anterior and posterior (femur) or medial and lateral (calcaneus) cortical bone in order to accentuate the arched trabecular patterns.

increase the risk of fragility fractures (Osborne et al., 1980; Lotz et al., 1995; Bell et al., 1999; Loveridge et al., 2004; Mayhew et al., 2005; Ryan and Krovitz, 2006; Manske et al., 2009; Djuric et al., 2010; Milovanovic et al., 2012). These considerations are also highly relevant in comparative studies that attempt to interpret load history of proximal femora of extinct and extant hominids and non-human anthropoids (Rafferty, 1998; Macchiarelli et al., 1999; Lovejoy et al., 2002; MacLatchy and Muller, 2002; Viola, 2002; Fajardo et al., 2007; Shaw and Ryan, 2012). In these studies of proximal femora, trabecular bone architectural patterns and variations are used to infer load history because in metaphyseal–epiphyseal regions they often seem more revealing and/or are better preserved than the histomorphology of the cortex. Consequently, these retrospective studies attempt to detect ontogenetic/phylogenetic patterns or changes in the load history of the proximal femur by considering potential functionally relevant associations in the spatial distributions of trabecular architectural characteristics.

Although the human femoral neck region is clearly complexly loaded (Lotz et al., 1995; Mourtada et al., 1996; Pidaparti and Turner, 1997; Rudman et al., 2006; Thomas et al., 2009), the stress transfer through this region is often simplified as a short cantilevered beam loaded in bending (Cristofolini et al., 1996; Martin et al., 1998; Demes et al., 2000; Lovejoy et al., 2002; Kaptoge et al., 2007; Skedros and Baucom, 2007). In turn, loading of this beam-like structure produces net tension in the superior aspect and net compression in the inferior aspect, with increased shear stresses in the middle region where longitudinal stresses are reduced (Pidaparti and Turner, 1997; Lovejoy, 2004). The arched trabecular patterns seen in anterior–posterior radiographs of the human proximal femur have traditionally been considered evidence supporting this load history (Skedros and Baucom, 2007; Skedros and Brand, 2011). However, additional specific trabecular architectural characteristics as possible correlates of habitual bending in this region have neither been clearly nor consistently demonstrated by many studies that have attempted to identify these in modern humans and in extinct and extant anthropoids (Rafferty, 1998; MacLatchy and Muller, 2002; Viola, 2002; Fajardo et al., 2007; Djuric et al., 2010; Ryan and Walker, 2010; Milovanovic et al., 2012; Shaw and Ryan, 2012). A significant challenge in these studies appears to be the lack of normative data from a 'control bone'; for example, a bone that is quasi beam-like, has similar arched trabecular patterns, and a known strain history (i.e., based on in vivo or ex vivo strain data).

In contrast to the human femoral neck where there are no in vivo strain gauge data, in vivo and rigorous ex vivo strain measurements on artiodactyl (e.g., sheep and deer) calcanei have shown comparatively simple uniaxial loading (Lanyon, 1973, 1974; Su et al., 1999). This relatively simple load history has stimulated investigations of sheep and deer calcanei in order to determine how they are adapted for habitual bending (i.e., bending that is stereotypical because it is spatially and temporally prevalent and predominant) (Skedros et al., 2004, 2007, 2009, 2012b). In his initial in vivo strain gauge studies of sheep calcanei, Lanyon (1973, 1974) drew comparisons of the stereotypical loading of this model to the human femoral neck because of their similar arched trabecular patterns, which also resemble tension and compression stress trajectories caused by bending (Figure 1). These and subsequent experimental studies of calcanei of deer and potoroos (an Australian marsupial) have shown that the direction of trabeculae in the arched dorsal and plantar tracts is closely aligned along the principal compressive and tensile strains, respectively (Biewener et al., 1996; Su et al., 1999). Extensive studies of cortical bone in sheep and deer calcanei have also shown that differences in dorsal versus plantar cortical thickness,[2] mineral content, and many histomorphological characteristics are correlated with differences in strain mode (e.g., tension, compression, and shear) and/or magnitude (where the magnitudes of ambient compression strains are much greater in the dorsal than plantar cortex) (Skedros et al., 1994a,b, 1997, 2004, 2007, 2009). For these reasons, the wild and domesticated artiodactyl calcaneus models seem ideal for studying trabecular and cortical bone adaptations for habitual bending.

Some investigators may ascribe strongly to the idea that interspecies differences can invalidate some comparisons of bone biology and biomechanics between artiodactyls and anthropoids. While this might seem to apply in some studies of cortical bone mechanical properties and histology (Currey, 1975, 2003), there are data showing that artiodactyl calcanei may be useful for these comparative studies because they have trabecular and cortical remodeling activities and dynamics that in many ways are similar to humans (Pastoureau et al., 1989; Newman et al., 1995; Skerry and Lanyon, 1995; Skedros et al., 2001; Turner, 2002; Zarrinkalam et al., 2009). Experimental studies have also shown that the mechanical properties of trabecular bone are generally similar in humans and bovines (Carter and Hayes, 1977; Lotz and Hayes, 1990; Keaveny et al., 1994b).

---

[2] For the purpose of clarity in discussing the results of the present investigation compared to results of past studies, the dorsal trabecular tract and dorsal cortex in most cases will be referred to as the 'compression' trabecular tract and 'compression' cortex, respectively, and the plantar trabecular tract and plantar cortex as the 'tension' trabecular tract and 'tension' cortex, respectively.

Table 1
Correlation rankings of trabecular architectural characteristics with mechanical parameters.

Rank	Liu et al. (2010) Trabecular bone stiffness	Diederichs et al. (2009) Maximum stress	Diederichs et al. (2009) Elastic modulus	Mittra et al. (2005) Ultimate compressive strength	Ulrich et al. (1999) Young's modulus [two characteristics]
1	SMI ($r = -0.90$) BV/TV ($r = 0.90$)	BV/TV ($r = 0.85$)	BV/TV ($r = 0.86$)	SMI ($r = -0.93$)	BV/TV, DA ($R^2 = 0.82$)
2	BS/BV ($r = -0.73$)	Tb.Th ($r = 0.61$)	Tb.Sp ($r = -0.58$)	BV/TV ($r = 0.90$)	BV/TV, Tb.N ($R^2 = 0.72$) BV/TV, Tb.Sp ($R^2 = 0.72$)
3	Tb.N ($r = 0.62$)	Tb.Sp ($r = -0.56$)	Tb.Th ($r = 0.57$)	Tb.Sp ($r = -0.83$)	BV/TV, Tb Th ($R^2 = 0.62$)
4	Tb.Sp ($r = -0.61$)	Tb.N ($r = 0.49$)	Tb.N ($r = 0.50$)	Tb.N ($r = 0.65$)	
5	Tb.Th ($r = 0.60$)			DA ($r = 0.50$)	
6				Tb.Th ($r = 0.45$)	
Species & Bone	Adult Human Distal Tibia	Adult Human Calcaneus	Adult Human Calcaneus	Adult Sheep Distal Femoral Condyles	Adult Human Femoral Head
Loading Method	Finite Element Model	Ex Vivo	Ex Vivo	Ex Vivo	Finite Element Model
Characteristics Not Measured*	–	DA; BS/BV; Conn. D; SMI	DA; BS/BV; Conn. D; SMI	BS/BV	BS/BV; Conn. D; SMI

DA = degree of anisotropy; BV/TV = bone volume fraction; BS/BV = bone surface density; Tb.Th = trabecular thickness; Tb.Sp = trabecular spacing; Tb.N = trabecular number; Conn.D = connectivity density; SMI = structure model index. * = characteristics not measured with respect to the present study. Data used are from the following studies of trabecular bone (Ulrich et al., 1999; Mittra et al., 2005; Diederichs et al., 2009; Liu et al., 2010). The 'sign' of the correlations in the Mittra et al. (2005) and Diederichs et al. (2009) studies was provided by written personal communications with the corresponding authors (January and February, 2012).

The present study focuses on quantifying regional variations in trabecular architecture in calcanei from wild deer and domesticated sheep as an initial step toward establishing these models as 'control bones' for studies examining the relationships between trabecular architectural characteristics and stress transfer in the hominid femoral neck. These models might also serve as 'control bones' for regions of bones from other anthropoid and non-anthropoid species that are thought to be, though to varying degrees, loaded in bending. Despite many studies of trabecular architectural characteristics of the human femoral neck (Whitehouse and Dyson, 1974; Carter et al., 1989; Lai et al., 2005; Blain et al., 2008; Liu et al., 2008; Jang and Kim, 2009; Thomas et al., 2009; Baum et al., 2010; Milovanovic et al., 2012), the only previous analysis that drew comparisons with artiodactyl calcanei was limited because only radiographs and two-dimensional measures were used (Skedros and Baucom, 2007). The present study advances this previous research by using micro-computed tomography (micro-CT), which has sufficient resolution for analyzing details of trabecular bone morphology (Fajardo and Muller, 2001; Fajardo et al., 2002; Ryan and Krovitz, 2006; Srinivasan et al., 2012).

Hypothesis and predictions

It is hypothesized that differences in specific architectural characteristics between dorsal 'compression' and plantar 'tension' trabecular tracts of artiodactyl calcanei will be identified, and that these differences will be consistent with those found in analyses of other bones known to experience habitual bending. This would support the mechanistic hypothesis that trabecular bone can adapt in specific ways in accordance with the locally prevalent/predominant strain mode and magnitude (typically highest strains are in the 'compression region' of the bone). These hypotheses are based on studies of bovine and human trabecular bone showing that:

(1) Energy absorption to yield, and ultimate and yield strengths are nearly 30% lower for tension versus compression loading (Keaveny et al., 1994a,b; Bayraktar et al., 2004),
(2) Trabecular bone is weakest in shear when compared with tension and compression (Mitton et al., 1997; Keaveny et al., 2001; Sanyal et al., 2012),
(3) Compressive yield strains (0.2% offset criterion) are higher than in tension (Keaveny et al., 1994b; Kopperdahl and Keaveny, 1998; Rincon-Kohli and Zysset, 2009; Wolfram et al., 2011),

(4) Microdamage initiation and propagation, and probably morphology, occur differently and asymmetrically in tension, compression, and shear (Nyman et al., 2009; Wu and Niebur, 2012), where yielding at local principal stresses occurs in the range of 88–121 MPa for compression and 35–43 MPa for tension (Nagaraja et al., 2005; Jungmann et al., 2011), and
(5) Trabecular architecture is highly sensitive to changes in prevalent/predominant load direction and magnitude (Pontzer et al., 2006; van der Meulen et al., 2006, 2009; Barak et al., 2011).

By focusing on the adaptability of specific trabecular architectural characteristics, we recognize that we do not account for the influences of local differences in cortical mass and other stress-carrying members (e.g., ligaments and tendons) on trabecular stresses and strains. While it is important to eventually account for these influences, there are data showing that specific/isolated trabecular architectural characteristics can explain significant proportions of variance in mechanical properties (Table 1) (Ulrich et al., 1999; Mittra et al., 2005; Diederichs et al., 2009; Liu et al., 2010). From this perspective, coupled with the mechanistic hypothesis, calcanei from domesticated sheep and wild deer were analyzed in terms of four predictions:

1. The mid-shaft will show dorsal/plantar architectural differences. In the mid-shaft, where the dorsal and plantar trabecular tracts begin to separate, this likely reflects a means for accommodating the intrinsic mechanical disparities in strain mode-specific loading that is linked to relatively simple bending in this location. (Here we adopt the view that enhancements will occur in the plantar 'tension' tract because of its comparatively deficient mechanical properties) (Table 2A).
2. The distal shaft will show fewer dorsal/plantar differences than the mid-shaft. In the distal shaft, where the dorsal and plantar tracts show extensive interconnections, this likely occurs as the consequence of locally increased trabecular mass compared to cortical mass, trabecular interconnectedness, and increased load complexity in the distal shaft, which would be expected to reduce differences in ambient strain magnitudes between the dorsal and plantar tracts.
3. The mid-shaft will show dorsal/middle/plantar architectural differences. The middle region between the dorsal and plantar tracts of the mid-shaft will show variations that likely reflect

Table 2
Predictions 1 and 3.

	A. Prediction 1			B. Prediction 3		
		Actual results			Actual results	
	Predictions	Deer	Sheep	Predictions	Deer	Sheep
DA	Dorsal < Plantar	D = P	D = P	M < D, P	M > D, P[a]	M = D, P
BV/TV	Dorsal < Plantar	D = P	D = P	M < D, P	M < D, P[a]	M < D, P[a]
BS/BV	Dorsal > Plantar	D = P	D > P[a]	M > D, P	M > D, P[a]	M > D, P[a]
Tb.Th	Dorsal < Plantar	D = P	D = P	M < D, P	M < D, P[a]	M < D, P[a]
Tb.Sp	Dorsal > Plantar	D = P	D < P	M > D, P	M > P	M, P > D[a]
Tb.N	Dorsal < Plantar	D < P[a]	D > P	M < D, P	M, P > D	D > M, P
Conn.D	Dorsal < Plantar	D = P	D > P	M < D, P	M > D, P	M, D > P
	Subset (n = 7)[b]	D < P[a]	D = P			
SMI	Dorsal > Plantar	D = P	D = P	M > D, P	M > D, P[a]	M > D, P[a]
	Subset (n = 7)[b]	D = P	D = P			

Mid-shaft only (where tracts begin to separate); Dorsal (D) = 'compression' and highest strain; Middle (M) = 'shear' and lowest strain; Plantar (P) = 'tension' and intermediate strain. Predictions are based on mechanical testing data from Keaveny et al. (1994a,b, 2001), Bayraktar et al. (2004), and Mittra et al. (2005). If we had adopted the alternative view that there would be greater enhancement in the 'compression regions', then the following characteristics would have been consistent with predictions (deer: none; sheep: Tb.Sp, Tb.N, and Conn.D).

[a] Prediction matches actual results.
[b] This analysis was conducted on subsets of data from similar sized VOIs.

low strains/stresses and/or the increased prevalence of shear stresses, as expected in neutral axis regions where the stress trajectories intersect (Table 2B).

4. The distal shaft will show fewer dorsal/middle/plantar differences than the mid-shaft. Compared with the mid-shaft, the distal shaft will show less distinct/consistent dorsal/middle/plantar variations as the likely consequence of more extensive trabecular interconnectedness, in addition to increased load complexity in the distal shaft.

Materials and methods

One calcaneus was obtained from each of 13 skeletally mature (two year old) female domesticated sheep (*Ovis aries*; breed is crossed Suffolk/Hampshire and Rambouillet) and from each of 13 mature (three−four years old) male wild Rocky Mountain mule deer (*Odocoileus hemionus hemionus*). The sheep were raised in paddocks where they were grown for human consumption. The deer were obtained from their natural habitat during a hunting season. All bones were screened for trauma and fractures during the butchering process. While the exact mass of each animal was not known, the ranges for the ages are known for the herds from which the animals were obtained (deer, 60−74 kg; sheep, 56−66 kg). The bones were dissected free of soft tissue. Biomechanical 'length' measurements were made from previously defined 0% (distal)−100% (proximal) aspects of the shaft, which correspond to the 'free' and 'fixed' ends of the bone, respectively (Skedros et al., 1994a). The 0% location was at the distal-dorsal 'notch' and the 100% was located at the center of the proximal articular surface (Figure 2A). As described below, segments from the 20, 30, 40 and 50% locations of the shaft were used. The 40 and 50% segment locations are considered to be from the 'mid-shaft', and the 20 and 30% segment locations are considered to be from the 'distal shaft' (Figure 2B).

In vivo and ex vivo studies of the artiodactyl calcaneus model

The in vivo strain data reported by Lanyon (1973, 1974) in domesticated sheep calcanei were obtained from varying lateral locations of the cortex while the animals walked and trotted. The ex vivo strain data in deer calcanei were obtained from bones that were loaded in a fixed position simulating mid-stance of walking and running gaits (Su, 1998; Su et al., 1999). In addition to influences of strain mode, we recognize that functional adaptation of some specific trabecular characteristics could be evoked by stress/strain magnitude (van der Meulen et al., 2009). When compared with the plantar aspect of these bones, stresses would be expected to be greatest in both the dorsal 'compression' trabecular tract and its adjacent cortex (Skedros et al., 2001). We also recognize that we are at risk of oversimplifying the load history of these bones because of the limited in vivo strain data for the sheep and the lack of in vivo strain data for the deer (discussed further below). Finally, indirect evidence supporting the probability that multidirectional stresses are relatively more prevalent in the distal shaft includes: (1) the reduced mineralization differences between the dorsal and plantar cortices toward the distal shaft (the peak difference is in the mid-shaft) (Skedros et al., 1994b), and (2) the comparatively circular cross-sectional shape of the distal shaft is a morphology that is commonly associated with the increased torsion seen toward the ends of bones (Currey, 2002; Zebaze et al., 2005). It is for these reasons that we stated different predictions for the mid-shaft versus distal shaft.

High resolution micro-computed tomography (micro-CT)

The bones were scanned using a GE Medical Systems EVS-RS9 micro-CT scanner (46.4 μm resolution, 80 kVp, 450 μA, and exposure time of 500 ms). All images included cortical and trabecular bone, and were exported as 16-bit VFF files. Image reconstructions were centered at 20, 30, 40, and 50% of the length of the intact shaft of each bone, and each reconstructed segment was 4 mm thick and spanned the entire transverse breadth of the bone. In each of the four segments, three volumes of interest (VOI) were selected: the dorsal, middle, and plantar regions in the trabecular envelope (Figure 2C). In these VOI all of the trabecular bone were sampled except for the bone within 0.5 mm from the cortex. The sizes of the VOI (mm³, mean ± standard deviation) are: (1) deer mid-shaft: dorsal (105 ± 40), middle (159 ± 35), and plantar (147 ± 35); (2) deer distal shaft: dorsal (201 ± 46), middle (274 ± 76), and plantar (297 ± 66); (3) sheep mid-shaft: dorsal (202 ± 65), middle (215 ± 37), and plantar (264 ± 75); and (4) sheep distal shaft: dorsal (314 ± 84), middle (300 ± 67), and plantar (340 ± 79).

Analysis of the scanned segments was conducted with commercially available software (General Electric (GE) Health Care MicroView version ABA 2). The eight trabecular architectural characteristics that were analyzed in each VOI (3 VOI/segment) are listed below. The degree of anisotropy (DA) was determined using QUANT3D software (IDL Virtual Machine; Boulder, Colorado, USA) in terms of the star volume distribution method as described elsewhere (Odgaard et al., 1997; Ketcham and Ryan, 2004). For this analysis, three additional and relatively smaller spherical VOI were selected within the larger volumes that were used to measure the other seven characteristics. These smaller VOI were also from the dorsal, middle, and plantar regions of each segment location. These VOI were 62 voxels in diameter (3.0 mm; edge of one voxel = 0.048 mm), and they were centered at 80% (dorsal), 50%, and 20% (plantar) of the medullary height, as measured in the sagittal plane.

The eight characteristics that were quantified included:

(1) Degree of anisotropy [DA (unitless); larger values = increased alignment of trabeculae],
(2) Bone volume fraction [BV/TV (%); bone volume ÷ total volume of VOI],
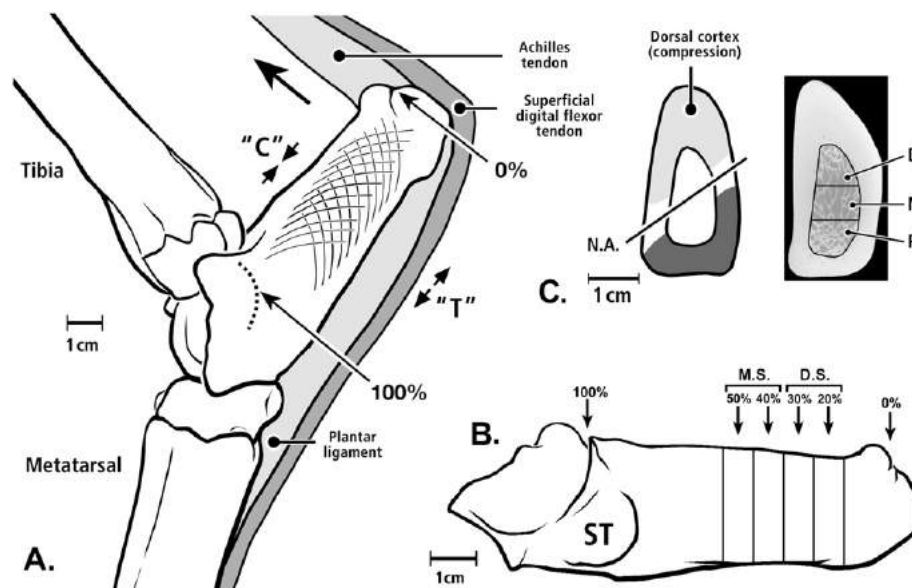
Figure 2. (A) Lateral-to-medial view of a left ankle of a skeletally mature mule deer showing locations for defining shaft 'length'. The large arrow shows the direction of force by the common calcaneal tendon in mid-stance, loading the dorsal cortex in compression ('C') and plantar cortex in tension ('T'). The arched trabecular patterns are shown in a stylized/simplified fashion (Su et al., 1999). (B) Medial-to-lateral view of a right deer calcaneus. M.S. = mid-shaft (40 and 50% segments); D.S. = distal shaft (20 and 30% segments); ST = sustentaculum talus. (C) As shown in the section from the 50% location, the neutral axis (N.A.) courses between the dorsal 'compression' and plantar 'tension' cortices and trabecular tracts. The actual CT image at far right shows the dorsal (D), middle (M), and plantar (P) locations of the VOIs within a 40% segment.

(3) Bone surface density [BS/BV (mm^{-1}), bone surface ÷ bone volume],
(4) Trabecular thickness [Tb.Th (mm)],
(5) Trabecular spacing [Tb.Sp (mm), average trabecular separation],
(6) Trabecular number [Tb.N (no. mm^{-1})],
(7) Connectivity density [Conn.D (no. mm^{-3}), density of interconnected trabeculae], and
(8) Structure model index [SMI (unitless); honeycomb-, plate-, or rod-like trabeculae].

Descriptions of these characteristics can be found in prior studies (Hildebrand and Ruegsegger, 1997a,b; Muller et al., 1998; Hildebrand et al., 1999; Fajardo and Muller, 2001; MacLatchy and Muller, 2002; Fajardo et al., 2007).

The SMI reflects the presence and distribution of trabecular morphologic types (Hildebrand and Ruegsegger, 1997b; Hildebrand et al., 1999). In an ideal plate-like structure the SMI value is 0, and in an ideal rod-like structure the SMI value is 3 (Hildebrand and Ruegsegger, 1997b). Negative SMI values represent low porosity concave plate-like structures resembling honeycombs, and are sometimes referred to as spherical voids or 'Swiss cheese' architecture (Hildebrand et al., 1999; Stauber and Muller, 2006). The degree of anisotropy (DA) measures trabecular alignment along a preferred axis. At values equal to 1 trabecular tissue is entirely isotropic (no preferred orientation) and as DA increases above 1 trabecular tissue becomes more anisotropic (i.e., more aligned) (Fajardo and Muller, 2001; Maga et al., 2006).

Statistical analysis

A three-way ANOVA design was used to assess effects and interactions between region, section location, and species. Paired *t*-tests were used for comparisons among dorsal, middle, and plantar regions at each section location (mid-shaft, distal shaft) within each species. Pearson correlation coefficients (*r* values) were determined to identify associations between pairs of the trabecular

architectural characteristics data, and between cortical thickness (Ct.Th) and each trabecular characteristic within each species. This was accomplished by comparing the trabecular architecture characteristics of the dorsal and plantar tracts to the thickness of their neighboring cortex. An alpha level of ≤0.05 was considered statistically significant.

Additional analyses were also conducted to determine if there are relationships between the sizes of the VOIs analyzed and each of the seven trabecular architectural characteristics (DA was not included because it was measured using a fixed VOI). These analyses were accomplished in three steps. First, Pearson correlation coefficients were determined for comparisons of each of the seven trabecular architectural characteristics with the VOIs from which they were obtained. Second, paired *t*-tests were used to determine if differences in the sizes of the VOIs of the dorsal and plantar tracts were statistically significant in the mid-shaft and distal shaft locations of each species. The middle regions were not included in this step in order to simplify the analysis. Third, subsets of seven VOIs from each of the dorsal and plantar tracts were obtained after paired comparisons showed that these subsets of dorsal versus plantar VOIs were *not* significantly different. Paired *t*-tests were then repeated to determine if the dorsal versus plantar difference (or similarity) of Conn.D and SMI obtained from these VOI subsets changed at the mid-shaft and distal shaft locations. Only Conn.D and SMI data were used in this final step because they: (1) are the only trabecular characteristics that (in step 1) showed correlations with VOI size (described below), and (2) are the trabecular characteristics analyzed in this study that are most likely to be influenced by VOI size variations (Kivell et al., 2011; Lazenby et al., 2011).

Results

Representative CT images of some of the cross-sections and VOIs from each species are shown in Figures 3 and 4. ANOVA results showed significant effects of shaft location and species for all characteristics measured. The effect of region is consistent with results of paired *t*-tests described below, which focus on the data in
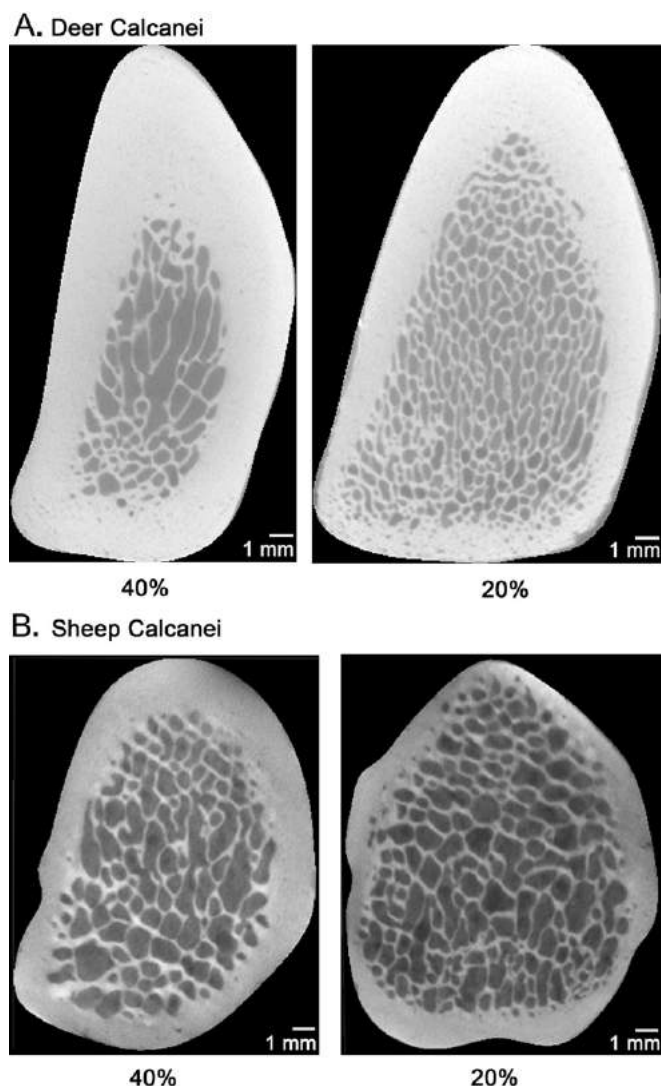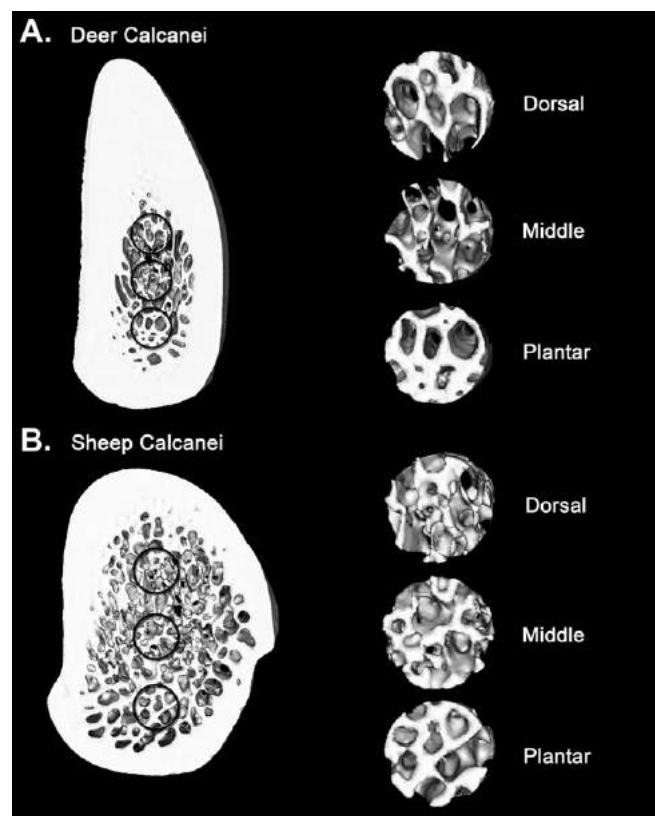
Figure 3. Transverse sections of (A) deer calcanei, and (B) sheep calcanei at 40 and 20% of shaft length. In each image, medial is to the left and plantar is toward the bottom. The images show the distal-most portion of the segment.

Figure 4. Micro-CT images showing volumes of interest (VOI) from the dorsal, middle, and plantar regions of (A) deer calcanei (40% location) and (B) sheep calcanei (40% location). These magnified VOIs (3 mm) at RIGHT are from within the cross-section at LEFT. The VOIs shown have equal size because they were used for the analysis of the degree of anisotropy (DA) where a fixed VOI size was employed. VOIs that were used to quantify the other seven architectural characteristics were adjusted to the size of the anatomical region being analyzed, as described in the text.

regions and shaft locations within each species (Table 3). Because many characteristics are interdependent as a result of their physical association, the correlation coefficients (Table 4) are considered primarily in terms of characteristics that are less interdependent. Results of correlations between trabecular architectural characteristics and nearby cortical thickness are shown in Table 5.

Additional analyses of potential effects of differences in VOI size

VOIs were significantly greater in the plantar tracts of both shaft locations in the deer calcanei and only in the mid-shaft location in sheep calcanei. Correlation analyses conducted between each of the seven trabecular architectural characteristics and VOI size of the dorsal tract, plantar tract, and middle regions showed that the only correlations that exceeded the absolute value of $r = 0.3$ occurred in the distal shaft of deer calcanei (Conn.D, $r = 0.36$; SMI, $r = 0.38$; p values < 0.005). SMI and Conn.D results from the subset ($n = 7$) of similarly sized VOIs from each dorsal and plantar tract of each shaft location of the deer calcanei indicate: (1) dorsal/plantar SMI data remained non-significant at both shaft locations (Table 2), (2) Conn.D became significantly greater in the plantar cortex of the

mid-shaft (it was a statistical trend at $p = 0.08$ when the entire data set was used) (Table 2), and (3) the dorsal/plantar difference in Conn.D at the distal shaft remained significant but the sign ('>' or '<') of this difference inverted (i.e., was plantar > dorsal, and became dorsal > plantar). The results of the final step of this analysis in sheep calcanei indicate that: (1) dorsal/plantar SMI data remained non-significant at both shaft locations (Table 2), (2) the dorsal/plantar difference in Conn.D at the mid-shaft became non-significant ($p = 0.1$) (Table 2), and (3) the dorsal/plantar difference in Conn.D at the distal shaft remained significant and the sign of the difference remained the same.

Prediction 1: the mid-shaft will show dorsal/plantar architectural differences

<u>Deer calcanei</u> When all data are considered, the only characteristic that differed in the manner predicted was Tb.N, which is greater in the plantar (tension) region ($p = 0.01$). In deer calcanei, the SMI values in dorsal (-2.62 ± 0.65) and plantar (-3.13 ± 0.39) regions are both indicative of honeycomb-like trabecular structure. Contrary to expectations in Prediction 1 (Table 2), the deer mid-shaft calcanei showed no statistical differences between dorsal and plantar tracts, and no significant differences that correspond with the sign ('>' or '<') of these expectations in the dorsal and plantar regions in terms of DA, BV/TV, BS/BV, Tb.Th, Tb.Sp, Conn.D, and SMI (Table 3A). Statistical trends were observed in Tb.Sp ($p = 0.08$) and Conn.D ($p = 0.08$), but because these are not

Table 3
Tabulated data for the trabecular bone analysis of: (A) 13 mule deer calcanei, and (B) 13 sheep calcanei. A. Deer calcanei *t*-test results [mean (standard error)]. B. Sheep calcanei *t*-test results [mean (standard error)].

	Mid-shaft (40–50% locations)			Distal shaft (20–30% locations)		
	Dorsal	Middle	Plantar	Dorsal	Middle	Plantar
A						
DA	4.99^M (0.31)	$6.09^{D, P}$ (0.66)	4.25^M (0.33)	5.18 (0.30)	5.44^P (0.61)	4.22^M (0.44)
BV/TV	0.54^M (0.03)	$0.34^{D, P}$ (0.01)	0.56^M (0.02)	0.54^M (0.01)	$0.42^{D, P}$ (0.01)	0.52^M (0.01)
BS/BV	5.59^M (0.37)	$9.33^{D, P}$ (0.30)	5.95^M (0.35)	7.72^M (0.37)	$11.09^{D, P}$ (0.22)	7.80^M (0.30)
Tb.Th	0.44^M (0.04)	$0.25^{D, P}$ (0.01)	0.41^M (0.05)	0.31^M (0.02)	$0.21^{D, P}$ (0.01)	0.31^M (0.02)
Tb.Sp	0.58 (0.06)	0.71^P (0.11)	0.47^M (0.03)	0.31 (0.02)	0.31 (0.02)	0.31 (0.02)
Tb.N	$\mathbf{1.46^{M, P}\ (0.06)}$	1.59^D (0.09)	$\mathbf{1.64^D\ (0.06)}$	2.04^M (0.06)	$2.33^{D, P}$ (0.06)	2.02^M (0.06)
Conn.D	2.16^M (0.21)	$4.42^{D, P}$ (0.45)	2.79^M (0.26)	$\mathbf{6.21^{M, P}\ (0.51)}$	$11.43^{D, P}$ (0.55)	$\mathbf{7.63^{D, M}\ (0.61)}$
SMI	-2.62^M (0.65)	$0.10^{D, P}$ (0.15)	-3.13^M (0.39)	-1.53^M (0.29)	$-0.12^{D, P}$ (0.21)	-1.10^M (0.25)
B						
DA	3.82 (0.24)	4.22 (0.61)	3.96 (0.20)	$\mathbf{4.16^{M, P}\ (0.20)}$	2.90^D (0.22)	$\mathbf{3.12^D\ (0.32)}$
BV/TV	0.45^M (0.01)	$0.35^{D, P}$ (0.01)	0.44^M (0.01)	$\mathbf{0.48^{M, P}\ (0.02)}$	$0.42^{D, P}$ (0.01)	$\mathbf{0.45^{D, M}\ (0.01)}$
BS/BV	$\mathbf{8.58^{M, P}\ (0.20)}$	$10.56^{D, P}$ (0.20)	$\mathbf{8.04^{D, M}\ (0.21)}$	$\mathbf{8.01^{M, P}\ (0.33)}$	9.62^D (0.33)	9.26^D (0.24)
Tb.Th	0.26^M (0.01)	$0.20^{D, P}$ (0.00)	0.27^M (0.01)	$\mathbf{0.28^{M, P}\ (0.01)}$	0.22^D (0.01)	$\mathbf{0.21^D\ (0.01)}$
Tb.Sp	$\mathbf{0.43^{M, P}\ (0.01)}$	0.50^D (0.02)	$\mathbf{0.50^D\ (0.03)}$	0.39 (0.02)	0.43^P (0.02)	0.40^M (0.02)
Tb.N	$\mathbf{1.92^{M, P}\ (0.03)}$	$1.84^{D, P}$ (0.04)	$\mathbf{1.74^{D, M}\ (0.03)}$	1.91^P (0.05)	1.97^P (0.04)	$\mathbf{2.06^{D, M}\ (0.04)}$
Conn.D	5.03^P (0.35)	4.71^P (0.37)	$\mathbf{3.38^{D, M}\ (0.27)}$	$\mathbf{5.02^{M, P}\ (0.40)}$	5.67^D (0.56)	6.07^D (0.37)
SMI	-0.40^M (0.18)	$0.16^{D, P}$ (0.12)	-0.60^M (0.17)	-1.04 (0.41)	-0.53^P (0.23)	-0.82^M (0.19)

Means and standard errors (SEM) are shown. The superscripted letters indicate statistical significance ($p \leq 0.05$) between the dorsal (D), middle (M) and plantar (P) VOIs. Bolded text = dorsal and plantar locations are statistically different ($p \leq 0.05$).

statistically significant they cannot be considered as corresponding to the sign of the predictions. The difference in Conn.D became significant (plantar > dorsal, as predicted) when the analysis used subset data from similar size VOIs.

Sheep calcanei Also contrary to expectations in Prediction 1 in sheep mid-shaft calcanei, there are no statistical differences (when all data are considered) between the dorsal and plantar regions in terms of DA, BV/TV, Tb.Th, and SMI. Furthermore, the statistically significant differences in Tb.Sp, Tb.N, and Conn.D are not consistent with the sign of the predictions (e.g., predicted Tb.N was dorsal < plantar; actual is dorsal > plantar) (Table 3B). Consequently, only BS/BV showed significant dorsal/plantar differences that were expected in the sheep mid-shaft calcaneus. Unlike the deer mid-shaft calcaneus where the dorsal and plantar SMI values showed honeycomb trabeculae, the sheep mid-shaft location showed SMI values in dorsal (-0.40 ± 0.18) and plantar (-0.60 ± 0.17) regions to have features of plates and honeycombs (Figure 5). As suggested by the correlation analyses (Table 4), these regional *and* species differences might reflect BV/TV variations (i.e., higher BV/TV in the deer, and regionally lower BV/TV in the middle regions of both species). Figure 6 shows that the SMI data from the middle regions of both species were obtained from VOIs that had relatively low BV/TV when compared to dorsal and plantar tracts. This helps to explain the lack of, or relatively low, correlations of SMI with BV/TV in the middle regions of mid-shaft locations of *both* species (Table 4).

The general conclusions do not change even if the expectations in Prediction 1 are reversed to conform to the alternative view that the relatively more highly stressed compression environment would show mechanical enhancements of trabecular bone. In this case, the deer mid-shaft shows a complete lack of correspondence (in Prediction 1 only Tb.N was consistent) and the sheep mid-shaft shows differences in Tb.Sp, Tb.N, and Conn.D instead of only BS/BV.

Prediction 2: the distal shaft will show fewer dorsal/plantar differences than the mid-shaft

The distal shaft of deer calcanei only showed one statistically significant dorsal/plantar difference (plantar > dorsal, Conn.D), but this significant difference inverted (dorsal > plantar) when the subset of VOIs of similar size was considered. These results do not provide strong support for the mid-shaft versus distal shaft comparison of Prediction 2 (i.e., more differences in the mid-shaft). The data in sheep calcanei also generally reject Prediction 2 by showing more dorsal versus plantar differences in the distal shaft than in the mid-shaft (six of eight characteristics versus four of eight characteristics, respectively).

Prediction 3: the mid-shaft will show dorsal/middle/plantar architectural differences

In both species (when all data are considered), five of eight characteristics showed the 'patterns' of the expected differences in Prediction 3 (Table 2). The exceptions included dorsal/middle/plantar patterns in DA, Tb.N, and Conn.D. ('Patterns' refers to instances when the middle region differs from the dorsal and plantar regions, regardless of whether or not the dorsal and plantar regions are significantly different.) The data therefore show that in the mid-shaft the middle region generally differs from the other two regions even though only one characteristic in each species showed a dorsal/plantar difference that satisfied Prediction 1.

Prediction 4: the distal shaft will show fewer dorsal/middle/plantar differences than mid-shaft

In the deer calcanei (when all data are considered), five of eight characteristics (BV/TV, BS/BV, Tb.Th, Conn.D, and SMI) showed similar patterns in differences of trabecular architectural characteristics between the dorsal/middle/plantar regions in both the mid-shaft and distal shaft, which is not consistent with Prediction 4. These results contrast with data in the sheep calcanei where only one of eight characteristics (BV/TV) showed the predicted dorsal/middle/plantar differences in the distal shaft when compared to five of eight found in the mid-shaft. The latter finding is consistent with Prediction 4.

Discussion

The architectural characteristics that have often been shown to be most important in conveying trabecular bone strength and stiffness (BV/TV, DA and SMI) did not significantly differ between the dorsal and

Table 4
Results of Pearson correlation analyses in (a) 13 deer calcanei, and (b) 13 sheep calcanei.

	DA	BV/TV	BS/BV	Tb.Th	Tb.Sp	Tb.N	Conn.D	SMI
a								
All Trabecular Locations								
DA								
BV/TV	−0.59							
BS/BV	0.37	−0.86						
Tb.Th	−0.40	0.80	−0.96					
Tb.Sp	0.55	−0.60						
Tb.N			0.44	−0.48	−0.59			
Conn.D		−0.43	0.72	−0.65		0.65		
SMI	0.52	−0.92	0.81	−0.69	0.44		0.55	
Dorsal								
DA								
BV/TV	−0.56							
BS/BV		−0.76						
Tb.Th		0.64	−0.92					
Tb.Sp	0.71	−0.64						
Tb.N					−0.70			
Conn.D			0.57			0.50‡		
SMI		−0.94	0.73	−0.54‡			0.48‡	
Middle								
DA								
BV/TV	−0.74							
BS/BV								
Tb.Th			−0.85					
Tb.Sp	0.57	−0.84						
Tb.N	−0.57	0.71	0.57		−0.79			
Conn.D	−0.58	0.70	0.48‡		−0.78	0.92		
SMI		−0.49‡						
Plantar								
DA								
BV/TV	−0.57							
BS/BV	0.52‡	−0.77						
Tb.Th		0.71	−0.95					
Tb.Sp								
Tb.N			0.86	−0.91	−0.50‡			
Conn.D	0.58		0.48‡		−0.55	0.56		
SMI	0.74	−0.75	0.75	−0.58			0.52‡	
b								
All Trabecular Locations								
DA								
BV/TV								
BS/BV		−0.84						
Tb.Th		0.77	−0.93					
Tb.Sp		−0.44						
Tb.N			0.33	−0.31‡	−0.89			
Conn.D			0.49	−0.40	−0.74	0.86		
SMI		−0.71	0.79	−0.56			0.50	
Dorsal								
DA								
BV/TV	0.49‡							
BS/BV	0.57	−0.84						
Tb.Th	−0.63	0.70	−0.74					
Tb.Sp								
Tb.N					−0.83			
Conn.D			0.50‡		−0.85	0.77		
SMI		−0.56	0.71				0.71	
Middle								
DA								
BV/TV								
BS/BV	0.56	−0.54‡						
Tb.Th			−0.58					
Tb.Sp		−0.69						
Tb.N		0.67			−0.97			
Conn.D		0.57			−0.84	0.84		
SMI			0.74					
Plantar								
DA								
BV/TV								
BS/BV		−0.70						
Tb.Th			−0.81					
Tb.Sp		−0.57						

Table 4 (*continued*)

	DA	BV/TV	BS/BV	Tb.Th	Tb.Sp	Tb.N	Conn.D	SMI
Tb.N			0.55	−0.75	−0.81			
Conn.D			0.69	−0.64		0.72		
SMI		−0.64	0.78					

These correlations were determined using data from the mid-shaft (40–50% locations).
‡ = statistical 'trends' with $p > 0.05$ and < 0.10. Correlation coefficients without superscript '‡' are $p \leq 0.05$.

plantar tracts in either species. This suggests that trabecular architectural characteristics, when considered in isolation, do not relate in obvious or expected ways with the non-uniform strain mode/magnitude distribution. Hence, none of the hypotheses are supported, meaning that simplistic interpretations of trabecular morphology are unsupported. As discussed below, the differences between species could be due to: (1) body size, (2) activity levels, (3) sex ratio of the samples, or (4) sizes of the VOI analyzed.

Comparisons with data in the femoral neck of humans and other anthropoids

Milovanovic et al. (2012) examined the entire inferior and superior portions of the trabecular bone of the femoral mid-neck of elderly female cadavers ($n = 14$; 74.1 ± 9.3 years) and showed that the inferior 'compression' region has greater BV/TV, Tb.Th, and DA ($p < 0.001$), and less rod-like trabeculae ($p = 0.047$), however, SMI values still exceed 2.0 in both superior and inferior regions.[3] Although these results support the common idea that regionally increased stresses result in preferential adaptation of the inferior 'compression' region (Carter et al., 1989; Lotz et al., 1995), our findings do not resemble these data, possibly because of the effect of age-related bone loss. By contrast, the youngest age group (20−39 years) in the human femoral neck study of Djuric et al. (2010) showed Tb.Th ($p = 0.05$) to be the only characteristic that is significantly different between the tracts (greater in 'compression region'). By contrast, this characteristic and all of the others measured (BV/TV, Tb.Sp, Tb.N, DA, SMI, and Conn.D) are significantly different between the tension and compression regions in the 40−59 year-old group.[4] It is likely that the post-maturation emergence of these differences reflects generally reduced loading with age and not some other volitional change in habitual load history. Consequently, the young/healthy femoral necks show only one difference (Tb.Th) between the compression and tension regions attributable to the non-uniform stress distribution and not to an aging effect. The deer calcaneus also showed only one difference (Tb.N) that is likely mechanically important (Mittra et al., 2005), however, this occurred in the 'tension tract'.

In a detailed micro-CT study, Fajardo et al. (2007) investigated trabecular architectural characteristics in the proximal femora from several extant and relatively young adult, non-human anthropoid species. Their study was also based on the presumption that bending occurs habitually in all of the bone regions studied. They also failed to find consistent differences in trabecular architectural characteristics (BV/TV, DA, SMI, Tb.N, Tb.Sp, Tb.Th, and Conn.D) between the superior and inferior aspects of the trabecular bone in the femoral necks.

---

[3] This statistical analysis, which is not reported in the original paper by Milovanovic et al. (2012), was provided by M. Djuric and P. Milovanovic by written communication in February 2012.

[4] This statistical analysis, which is not reported in the original paper by Djuric et al. (2010), was provided by M. Djuric and P. Milovanovic by written communication in February 2012.

Table 5
Correlations of architectural characteristics with cortical thickness (each trabecular tract compared to its adjacent cortex) in (A) 13 deer calcanei, and (B) 13 sheep calcanei.

|	DA	BV/TV	BS/BV	Tb.Th	Tb.Sp	Tb.N	Conn.D	SMI
A. Deer Calcanei								
Mid-shaft								
Ct.Th	0.41							
Distal Shaft								
Ct.Th							−0.49	
B. Sheep Calcanei								
Mid-shaft								
Ct.Th		0.46			−0.54	0.54	0.39	
Distal Shaft								
Ct.Th		0.43	−0.54	0.64		−0.46	−0.39	−0.44

[Dorsal and plantar regions only; Coefficients shown are $p < 0.05$].
Ct.Th = cortical thickness; see Methods section for other abbreviations.

In summary, even in view of non-age-related differences in trabecular architectural characteristics that have been reported in mature anthropoid proximal femora these studies fail to find consistent correlations between trabecular architectural characteristics and the presumed non-uniform load environment. Similar confusing/inconsistent results have been reported in other studies of human and non-human proximal femora that are also often couched in terms of the traditional context of Wolff's law, where high stresses in the 'compression region' are expected to correlate with trabecular bone with clearly enhanced mechanical properties: more dense (reduced porosity), highly oriented, and extensively interconnected (Rafferty, 1998; MacLatchy and Muller, 2002; Viola, 2002; Ryan and Walker, 2010; Shaw and Ryan, 2012). In these perspectives, the influences of developmental constraints on trabecular architectural variations within and between bones should be considered (Swartz et al., 1998; Byers et al., 2000; Nafei et al., 2000; Skedros and Baucom, 2007).

Additional limitations and confounding issues when comparing artiodactyls and primates

Experimental studies have shown that the mechanical properties of trabecular bone are generally similar in humans and bovines (Carter and Hayes, 1977; Lotz and Hayes, 1990; Keaveny et al., 1994b). When differences occur, they are often a function of relatively greater BV/TV in these non-human species, as has been reported in ovines and cervines (present study; Mittra et al., 2005) and bovines (Carter and Hayes, 1977; Rice et al., 1988; Keaveny et al., 1994b). Variations in BV/TV can also be associated with differences in other mechanically important architectural characteristics (e.g., SMI and Tb.N). Nevertheless, relatively high absolute values of BV/TV and SMI that we found in the trabecular tracts of sheep and deer calcanei resemble those reported in younger humans and in older humans in some locations (e.g., in the femoral neck where the tracts merge beneath the femoral head) (Lotz and Hayes, 1990; Hildebrand et al., 1999). Inter-species comparisons of trabecular architecture and mechanical properties can be drawn between artiodactyls and anthropoids as long as the effects that BV/TV variation might have on other architectural characteristics are considered.

Scaling relationships between animal size and trabecular architecture are also important considerations when comparing artiodactyls with primates, especially in view of the broad range of sizes of the primates that have been used in studies of trabecular bone architecture (Rafferty, 1998; MacLatchy and Muller, 2002; Viola, 2002; Lai et al., 2005; Fajardo et al., 2007; Djuric et al., 2010; Ryan and Walker, 2010; Milovanovic et al., 2012; Shaw and Ryan, 2012). For example, when compared with the estimated masses of our animals (male mule deer, 60–74 kg; female sheep, 56–66 kg), the masses of primates studied by Fajardo et al. (2007) are much less
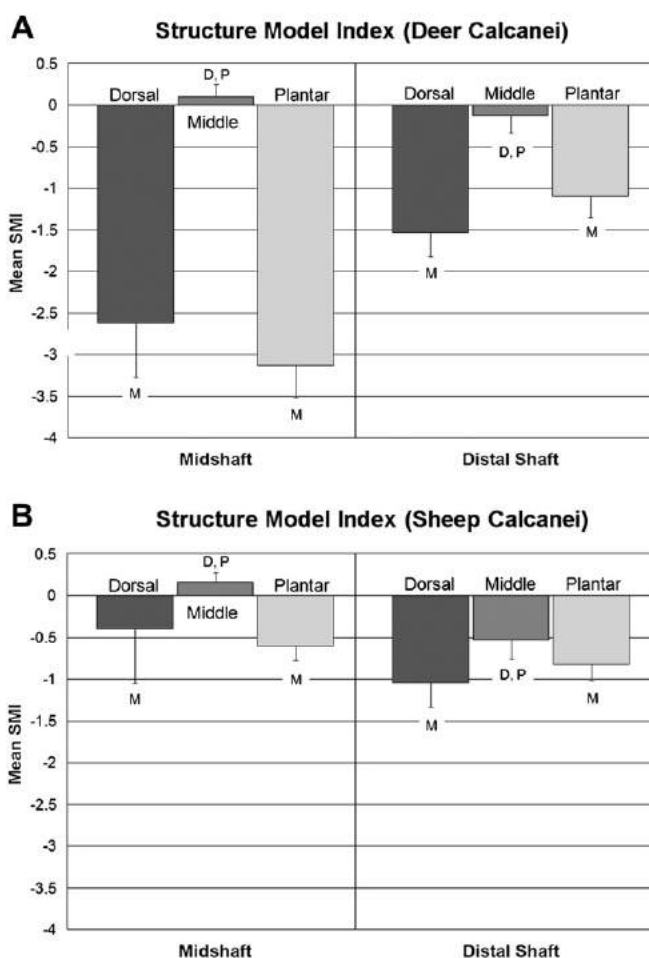
Figure 5. Structure model index (SMI) measurements for the (A) deer calcanei ($n = 13$), and (B) sheep calcanei ($n = 13$) showing negative values (honeycomb morphology) in most regions. Exceptions include the more plate-like morphology in the middle aspects of the mid-shafts of sheep and deer calcanei, and in the distal-middle aspect of deer calcanei. The letters below or above the bars indicate statistical significance ($p \leq 0.05$) between the dorsal (D), middle (M) and plantar (P) VOIs within the mid-shaft (left side) or distal shaft (right side).

(range: 3.6 (*Macaca fascicularis*; female)–11.9 kg (*Symphalangus syndactylus*; male)). By contrast, our animals are more similar to the mass ranges of typical adult chimpanzees (33–60 kg) and humans (36–78 kg) (Smith and Jungers, 1997). While Doube et al. (2011) have shown that trabecular BV/TV does not scale substantially with animal size in femora from a broad size range of various species (72 terrestrial mammals, 18 avians, and 1 crocodilian), their data revealed that trabeculae in larger animals' femora are thicker (Tb.Th), further apart (Tb.Sp) and fewer per unit number (Tb.N). This issue exposes an important consideration when drawing comparisons between our data and smaller primates, especially because Tb.N is the parameter that is most likely to be biomechanically significant in the dorsal/plantar comparisons in the deer calcanei (Mittra et al., 2005; Stauber et al., 2006; Badiei et al., 2007; Saparin et al., 2011). Another limitation of the present study is that all of the deer are male and the sheep are female. Sexual dimorphism might also help to explain why there are differences in trabecular bone between these species (Wang et al., 2010).

Ensuring that VOIs scaled to body size are used is also important for avoiding over-sampling in smaller- versus larger-bodied taxa, and in comparisons of regions that are not functionally homologous (Lazenby et al., 2011). Our smallest VOI is 3.5 times smaller than the
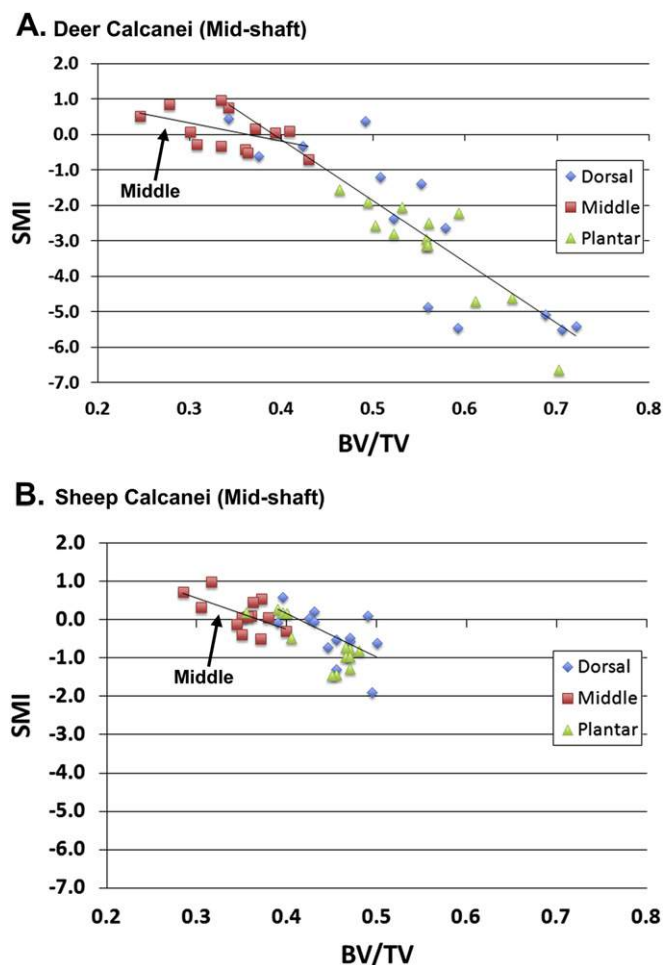
Figure 6. Scatter plots and least-squares regression lines for SMI versus BV/TV comparisons in mid-shaft locations of (A) 13 deer calcanei, and (B) 13 sheep calcanei. The data for the middle regions are relatively confined toward the upper left portions of the plots. The regression lines for the plantar tracts are not shown so that the differences between middle regions and dorsal tracts can be seen more clearly. The dorsal and plantar tracts have similar negatively sloping regression lines.

biggest VOI (105 mm^3 versus 340 mm^3). Thus, it was important to determine if the data could be biased by VOI size. Prior studies have shown that of the eight characteristics that we examined, SMI and Conn.D are the two that would most likely be influenced by VOI size (Kivell et al., 2011; Lazenby et al., 2011). This might explain the observation that the smallest VOIs (deer mid-shaft) also tend to have the lowest Conn.D (Table 3A). However, besides Conn.D data becoming statistically significant and consistent with predictions in the mid-shaft deer calcanei (superscripts in Table 2), there were no substantial changes in the conclusions that are based on comparisons made using Conn.D and SMI data from VOIs with similar sizes.

Inter-species comparisons could also be confounded by the relatively greater amount of cortical mass (as a percentage of the entire cross-section) that the artiodactyl calcaneal shaft has when compared with some anthropoid proximal femora, especially modern humans (Ohman et al., 1997; Rafferty, 1998; Ruff et al., 1999; Lovejoy et al., 2002; Mayhew et al., 2005). Support for this possibility includes finite element analyses of a young adult human distal radius and experimental studies of adult human femoral necks (ages: 59–83 years) show that reductions in trabecular bone mass have a much lesser effect on the overall bone strength than reductions in cortical mass (Pistoia et al., 2003; Holzer et al., 2009). Inter-species differences in limb morphology also likely have

important roles in the differences in the load sharing that occurs for primate proximal femora when compared with artiodactyl calcanei. For example, toward the distal ends of artiodactyl limb bones, including the calcanei, the potential for the modification of strains by local contractions of adjacent muscles is lacking when compared with primate limbs. These considerations are relevant for the present study because it is likely that there is disproportionately greater load sharing between the robust cortex and trabecular bone in artiodactyl calcanei than generally in proximal primate femora because of the potential for significant local muscle influences in the hip region. However, this distinction seems less important when considered in terms of two main findings of this study.

First, in deer calcanei the correlation analyses between the local cortical thickness and each of the trabecular architectural characteristics in the adjacent tract showed that only one characteristic correlated at each of the shaft locations (Table 5A). Also, while there are several significant correlations in the sheep calcanei these are inconsistent when compared with the deer calcanei (Table 5B). Second, the less robust cortex at the distal-most location of the calcaneal shaft that we measured more closely resembles the neck locations of chimpanzee and human proximal femora. For example, the cortical robusticity of the 20% and 30% locations of the sheep and deer calcanei are between the base- and mid-neck sections of the adult chimpanzee and human femora used in our prior study (Skedros and Baucom, 2007) (Figure 7). These data and observations suggest that the cortices of the artiodactyl calcanei do not have an important role in influencing their trabecular architecture as might have been anticipated. Additional analyses that consider cortical bone distribution across and along the entire shaft (e.g., second moments of area) are needed to rigorously examine these issues.

A more important factor in the inter-species differences in these correlations of cortical thickness with trabecular architecture might be the extent of the animal's general physical activity, which might explain the mixed findings in the calcanei of the relatively less active sheep (Table 5B versus A). There are data suggesting that wild deer are more physically active than domesticated sheep. For example, calcanei of mule deer have substantially higher concentrations of in vivo microdamage *and* dramatic histomorphological differences between their dorsal/plantar cortices (Skedros et al., 2011b). Increased activity might also explain why the deer calcanei have a dorsal/plantar difference (Tb.N) that is likely mechanically important.

Future studies of the artiodactyl calcaneus model as a 'control' for anthropoid bone adaptation

Anthropologists might wonder what would be the purpose of pursuing future studies of the artiodactyl calcaneus model for studies of anthropoid bones if there are so many factors that differ between these taxa. A series of studies has shown that the answer to this is clear when histomorphological characteristics of *cortical* bone are used to study adaptation for bending (Skedros et al., 2004, 2007, 2009, 2011a, 2012a, 2013). These studies have shown highly consistent patterns of histomorphological adaptation for bending in cortices of limb bones of horses, artiodactyls, chimpanzees, and modern humans. However, the role of this model is less clear for understanding trabecular bone adaptation in the anthropoid limb skeleton. We believe that the potential for this model will eventually be clear in positive ways that were not identified in this study. For example, there could be material characteristics of trabecular bone (e.g., lamellations, 'packets', and micromineralization patterns in individual struts) that more strongly correlate with a habitual bending history than architectural characteristics (Ciarelli et al., 2009; Skedros et al., 2012b). Synergism of material and architectural characteristics that are aimed at enhancing trabecular bone mechanical properties for local load environments is
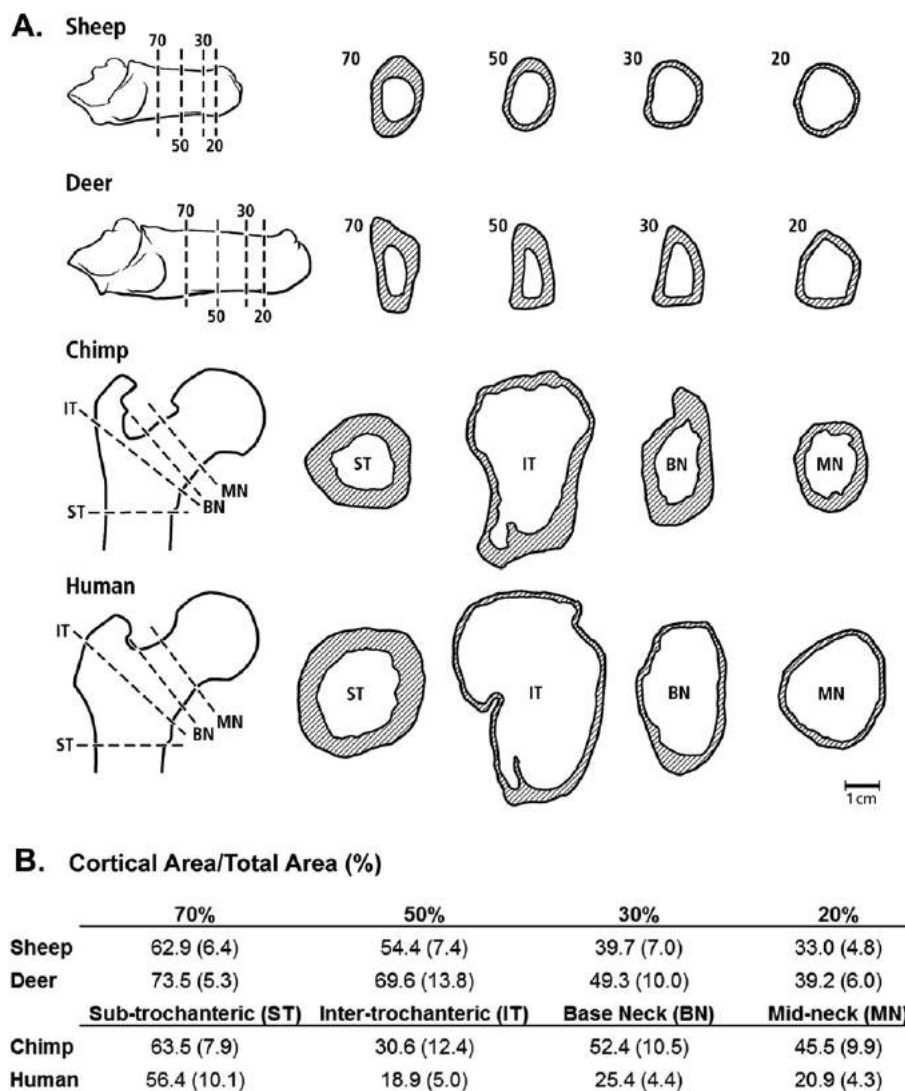
Figure 7. A. Medial-to-lateral views of drawings of adult sheep and deer calcanei, and anterior-to-posterior views of drawings of adult proximal chimpanzee and modern human femora. In the sheep and deer calcanei the section locations that are shown were defined using the same methods in the present study (70% = proximal shaft; 50% = mid-shaft, and 30-20% = distal shaft). These are representative sections from bones that were used in prior studies (40% locations were not obtained) where some of the calcanei were from the contralateral bone from the paired calcanei used in the present study: deer calcanei (n = 15), sheep calcanei (n = 15), chimpanzee femora (n = 8), and modern human femora (n = 15) (Skedros et al., 2001, 2004, 2012b; Skedros and Baucom, 2007). In the femora the abbreviations are: ST = subtrochanteric, IT = intertrochanteric, BN = base neck, MN = mid-neck. With the exception of the ST and 70% locations, the medullary cavities are completely filled with trabecular bone. The scale bar refers to the cross-sections. B. Cortical robusticity data (means and standard deviations) expressed as the percentage of cortical area (CA) with respect to the total area (TA) of the cross-section ((CA/TA)·100).

B. Cortical Area/Total Area (%)

	70%	50%	30%	20%
Sheep	62.9 (6.4)	54.4 (7.4)	39.7 (7.0)	33.0 (4.8)
Deer	73.5 (5.3)	69.6 (13.8)	49.3 (10.0)	39.2 (6.0)
	Sub-trochanteric (ST)	Inter-trochanteric (IT)	Base Neck (BN)	Mid-neck (MN)
Chimp	63.5 (7.9)	30.6 (12.4)	52.4 (10.5)	45.5 (9.9)
Human	56.4 (10.1)	18.9 (5.0)	25.4 (4.4)	20.9 (4.3)

an intriguing possibility that warrants study (Wang et al., 2012). We predict that trabecular material and architectural data can be considered in creative ways that will prove to be strong correlates of load history. This might mean considering measures of trabecular and cortical bone structure and histomorphology. Some trabecular architectural characteristics could also be considered in more detail. For example, SMI data revealed plate-like trabeculae in the middle regions of both species. Because the middle trabecular region is in the vicinity of the neutral axis, it likely experiences relatively greater shear stress than other regions (Young, 1989). Plate-like trabeculae might accommodate these locally prevalent/ increased shear stresses (Giesen and van Eijden, 2000). We could not locate any micro-CT studies that specifically evaluated trabecular morphologies in 'neutral axis regions' of anthropoid bones in order to determine if plate-like trabeculae are prevalent there. In these perspectives, the potential for artiodactyl calcanei as 'controls' holds promise for studies of trabecular bone in anthropoid bones.

This study helps to chart the course for future investigations that are essential for further developing sheep and deer calcanei as models for studying bone adaptation. These include: (1) in vivo studies of the strain environments in the cortical and trabecular envelopes, and finite element analyses based on these strain data, (2) mechanical testing studies coupled with multiple-variable regression analyses that consider the influence of histomorphological, compositional, and architectural characteristics of the tested specimens, and (3) incorporating in these analyses the mechanical influences of cross-sectional moments of area and asymmetrical cortical mass distributions and histomorphology along the calcaneal shaft in addition to the load-sharing functions of the nearby plantar ligament and flexor tendon. Ontogenetic and aging studies will also help to determine the relative importance of functional loading and developmental constraints in the emergence and maintenance of the trabecular morphology of the calcaneal shaft. The wild deer calcaneus model is less useful for these studies because their natural lifespan is likely insufficient to expose these effects, but studies of

post-menopausal osteoporosis and aging are possible in sheep (Turner, 2002; Zarrinkalam et al., 2009).

Conclusion

Among the eight trabecular architectural characteristics examined, Tb.N (and Conn.D in the subset analysis) showed the most obvious and potentially mechanically relevant regional differences between the dorsal and plantar tracts. This dorsal/ plantar Tb.N difference was found in the deer calcaneus (plantar > dorsal) but was opposite, and statistically significant, in the sheep calcaneus (dorsal > plantar). However, sheep calcanei did not show significant differences in Conn.D in the subset analysis. Regional differences in Tb.N, Conn.D and other trabecular architectural characteristics also have not been consistently found in previous studies of various anthropoid proximal femora where bending is considered the habitual load history. This is the case regardless of whether specific trabecular architectural variations are considered to enhance mechanical properties for high versus low stress, or for compression versus tension environments. In both species, significant differences in SMI were also found in the middle ('neutral axis') regions when compared with the neighboring tracts, and these differences are more dramatic in the deer calcanei. Studies are needed to determine if similar regional variations are found in anthropoid femoral necks that experience habitual bending.

The results of this study also reveal additional issues that must be considered in order to gain a more complete understanding of the potential mechanobiological relationships between hierarchical tissue organization and load histories of the artiodactyl calcaneus model. As long as influences of load sharing with the cortex and musculotendinous structures, animal mass, sexual dimorphism, scaling issues, and variations in VOI size are minimized or accounted for, these considerations also apply to anthropoid proximal femora and other bones where trabecular structural anisotropy suggests habitual bending. However, in view of available data, the use of the artiodactyl calcaneus as a potential 'control bone' cautions against simple interpretations of trabecular bone adaptation in the anthropoid femoral neck.

References

Adachi, J.D., Adami, S., Gehlbach, S., Anderson Jr., F.A., Boonen, S., Chapurlat, R.D., Compston, J.E., Cooper, C., Delmas, P., Diez-Perez, A., Greenspan, S.L., Hooven, F.H., LaCroix, A.Z., Lindsay, R., Netelenbos, J.C., Wu, O., Pfeilschifter, J., Roux, C., Saag, K.G., Sambrook, P.N., Silverman, S., Siris, E.S., Nika, G., Watts, N.B., 2010. Impact of prevalent fractures on quality of life: baseline results from the global longitudinal study of osteoporosis in women. Mayo Clin. Proc. 85, 806–813.
Badiei, A., Bottema, M.J., Fazzalari, N.L., 2007. Influence of orthogonal overload on human vertebral trabecular bone mechanical properties. J. Bone Miner. Res. 22, 1690–1699.
Barak, M.M., Lieberman, D.E., Hublin, J.J., 2011. A Wolff in sheep's clothing: trabecular bone adaptation in response to changes in joint loading orientation. Bone 49, 1141–1151.
Baum, T., Carballido-Gamio, J., Huber, M.B., Muller, D., Monetti, R., Rath, C., Eckstein, F., Lochmuller, E.M., Majumdar, S., Rummeny, E.J., Link, T.M., Bauer, J.S., 2010. Automated 3D trabecular bone structure analysis of the proximal femur – prediction of biomechanical strength by CT and DXA. Osteoporos. Int. 21, 1553–1564.
Bayraktar, H.H., Morgan, E.F., Niebur, G.L., Morris, G.E., Wong, E.K., Keaveny, T.M., 2004. Comparison of the elastic and yield properties of human femoral trabecular and cortical bone tissue. J. Biomech. 37, 27–35.
Bell, K.L., Loveridge, N., Power, J., Garrahan, N., Meggitt, B.F., Reeve, J., 1999. Regional differences in cortical porosity in the fractured femoral neck. Bone 24, 57–64.
Biewener, A.A., Fazzalari, N.L., Konieczynski, D.D., Baudinette, R.V., 1996. Adaptive changes in trabecular architecture in relation to functional strain patterns and disuse. Bone 19, 1–8.
Blain, H., Chavassieux, P., Portero-Muzy, N., Bonnel, F., Canovas, F., Chammas, M., Maury, P., Delmas, P.D., 2008. Cortical and trabecular bone distribution in the femoral neck in osteoporosis and osteoarthritis. Bone 43, 862–868.
Boonen, S., Autier, P., Barette, M., Vanderschueren, D., Lips, P., Haentjens, P., 2004. Functional outcome and quality of life following hip fracture in elderly women: a prospective controlled study. Osteoporos. Int. 15, 87–94.
Byers, S., Moore, A.J., Byard, R.W., Fazzalari, N.L., 2000. Quantitative histomorphometric analysis of the human growth plate from birth to adolescence. Bone 27, 495–501.
Carter, D.R., Hayes, W.C., 1977. The compressive behavior of bone as a two-phase porous structure. J. Bone Joint Surg. Am. 59, 954–962.
Carter, D.R., Orr, T.E., Fyhrie, D.P., 1989. Relationships between loading history and femoral cancellous bone architecture. J. Biomech. 22, 231–244.
Ciarelli, T.E., Tjhia, C., Rao, D.S., Qiu, S., Parfitt, A.M., Fyhrie, D.P., 2009. Trabecular packet-level lamellar density patterns differ by fracture status and bone formation rate in white females. Bone 45, 903–908.
Cristofolini, L., Viceconti, M., Cappello, A., Toni, A., 1996. Mechanical validation of whole bone composite femur models. J. Biomech. 29, 525–535.
Currey, J.D., 1975. The effects of strain rate, reconstruction and mineral content on some mechanical properties of bovine bone. J. Biomech. 8, 81–86.
Currey, J.D., 2002. Bones: Structure and Mechanics. Princeton University Press, Princeton.
Currey, J.D., 2003. The many adaptations of bone. J. Biomech. 36, 1487–1495.
Demes, B., Jungers, W.L., Walker, C., 2000. Cortical bone distribution in the femoral neck of strepsirhine primates. J. Hum. Evol. 39, 367–379.
Diederichs, G., Link, T.M., Kentenich, M., Schwieger, K., Huber, M.B., Burghardt, A.J., Majumdar, S., Rogalla, P., Issever, A.S., 2009. Assessment of trabecular bone structure of the calcaneus using multi-detector CT: correlation with microCT and biomechanical testing. Bone 44, 976–983.
Djuric, M., Djonic, D., Milovanovic, P., Nikolic, S., Marshall, R., Marinkovic, J., Hahn, M., 2010. Region-specific sex-dependent pattern of age-related changes of proximal femoral cancellous bone and its implications on differential bone fragility. Calcif. Tissue Int. 86, 192–201.
Doube, M., Klosowski, M.M., Wiktorowicz-Conroy, A.M., Hutchinson, J.R., Shefelbine, S.J., 2011. Trabecular bone scales allometrically in mammals and birds. Proc. R. Soc. B Biol. Sci. 278, 3067–3073.
Fajardo, R.J., Muller, R., 2001. Three-dimensional analysis of nonhuman primate trabecular architecture using micro-computed tomography. Am. J. Phys. Anthropol. 115, 327–336.
Fajardo, R.J., Ryan, T.M., Kappelman, J., 2002. Assessing the accuracy of high-resolution X-ray computed tomography of primate trabecular bone by comparisons with histological sections. Am. J. Phys. Anthropol. 118, 1–10.
Fajardo, R.J., Muller, R., Ketcham, R.A., Colbert, M., 2007. Nonhuman anthropoid primate femoral neck trabecular architecture and its relationship to locomotor mode. Anat. Rec. 290, 422–436.
Giesen, E.B., van Eijden, T.M., 2000. The three-dimensional cancellous bone architecture of the human mandibular condyle. J. Dent. Res. 79, 957–963.
Hildebrand, T., Ruegsegger, P., 1997a. A new method for the model-independent assessment of thickness in three-dimensional images. J. Microsc. 185, 67–75.
Hildebrand, T., Ruegsegger, P., 1997b. Quantification of bone microarchitecture with the structure model index. Comput. Methods Biomech. Biomed. Eng. 1, 15–23.
Hildebrand, T., Laib, A., Muller, R., Dequeker, J., Ruegsegger, P., 1999. Direct three-dimensional morphometric analysis of human cancellous bone: microstructural data from spine, femur, iliac crest, and calcaneus. J. Bone Miner. Res. 14, 1167–1174.
Holzer, G., von Skrbensky, G., Holzer, L.A., Pichl, W., 2009. Hip fractures and the contribution of cortical versus trabecular bone to femoral neck strength. J. Bone Miner. Res. 24, 468–474.
Jang, I.G., Kim, I.Y., 2009. Computational simulation of trabecular adaptation progress in human proximal femur during growth. J. Biomech. 42, 573–580.
Jungmann, R., Szabo, M.E., Schitter, G., Tang, R.Y., Vashishth, D., Hansma, P.K., Thurner, P.J., 2011. Local strain and damage mapping in single trabeculae during three-point bending tests. J. Mech. Behav. Biomed. 4, 523–534.
Kaptoge, S., Jakes, R.W., Dalzell, N., Wareham, N., Khaw, K.T., Loveridge, N., Beck, T.J., Reeve, J., 2007. Effects of physical activity on evolution of proximal femur structure in a younger elderly population. Bone 40, 506–515.
Keaveny, T.M., Guo, X.E., Wachtel, E.F., McMahon, T.A., Hayes, W.C., 1994a. Trabecular bone exhibits fully linear elastic behavior and yields at low strains. J. Biomech. 27, 1127–1136.
Keaveny, T.M., Wachtel, E.F., Ford, C.M., Hayes, W.C., 1994b. Differences between the tensile and compressive strengths of bovine tibial trabecular bone depend on modulus. J. Biomech. 27, 1137–1146.
Keaveny, T.M., Morgan, E.F., Niebur, G.L., Yeh, O.C., 2001. Biomechanics of trabecular bone. Annu. Rev. Biomed. Eng. 3, 307–333.

Ketcham, R.A., Ryan, T.M., 2004. Quantification and visualization of anisotropy in trabecular bone. J. Microsc. 213, 158–171.

Kivell, T.L., Skinner, M.M., Lazenby, R., Hublin, J.J., 2011. Methodological considerations for analyzing trabecular architecture: an example from the primate hand. J. Anat. 218, 209–225.

Kopperdahl, D.L., Keaveny, T.M., 1998. Yield strain behavior of trabecular bone. J. Biomech. 31, 601–608.

Lai, Y.M., Qin, L., Yeung, H.Y., Lee, K.K., Chan, K.M., 2005. Regional differences in trabecular BMD and micro-architecture of weight-bearing bone under habitual gait loading – a pQCT and microCT study in human cadavers. Bone 37, 274–282.

Lanyon, L.E., 1973. Analysis of surface bone strain in the calcaneus of sheep during normal locomotion. Strain analysis of the calcaneus. J. Biomech. 6, 41–46.

Lanyon, L.E., 1974. Experimental support for the trajectorial theory of bone structure. J. Bone Joint Surg. Br. 56, 160–166.

Lazenby, R.A., Skinner, M.M., Kivell, T.L., Hublin, J.J., 2011. Scaling VOI size in 3D μCT studies of trabecular bone: a test of the over-sampling hypothesis. Am. J. Phys. Anthropol. 144, 196–203.

Liu, X.S., Sajda, P., Saha, P.K., Wehrli, F.W., Bevill, G., Keaveny, T.M., Guo, X.E., 2008. Complete volumetric decomposition of individual trabecular plates and rods and its morphological correlations with anisotropic elastic moduli in human trabecular bone. J. Bone Miner. Res. 23, 223–235.

Liu, X.S., Zhang, X.H., Sekhon, K.K., Adams, M.F., McMahon, D.J., Bilezikian, J.P., Shane, E., Guo, X.E., 2010. High-resolution peripheral quantitative computed tomography can assess microstructural and mechanical properties of human distal tibial bone. J. Bone Miner. Res. 25, 746–756.

Lotz, J.C., Hayes, W.C., 1990. The use of quantitative computed tomography to estimate risk of fracture of the hip from falls. J. Bone Joint Surg. Am. 72, 689–700.

Lotz, J.C., Cheal, E.J., Hayes, W.C., 1995. Stress distributions within the proximal femur during gait and falls: implications for osteoporotic fracture. Osteoporos. Int. 5, 252–261.

Lovejoy, C.O., 1988. Evolution of human walking. Sci. Am. 259, 118–125.

Lovejoy, C.O., 2004. The natural history of human gait and posture. Part 2. Hip and thigh. Gait Posture 21, 113–124.

Lovejoy, C.O., Meindl, R.S., Ohman, J.C., Heiple, K.G., White, T.D., 2002. The Maka femur and its bearing on the antiquity of human walking: applying contemporary concepts of morphogenesis to the human fossil record. Am. J. Phys. Anthropol. 119, 97–133.

Lovejoy, C.O., McCollum, M.A., Reno, P.L., Rosenman, B.A., 2003. Developmental biology and human evolution. Annu. Rev. Anthropol. 32, 85–109.

Loveridge, N., Power, J., Reeve, J., Boyde, A., 2004. Bone mineralization density and femoral neck fragility. Bone 35, 929–941.

Ma, R.S., Gu, G.S., Huang, X., Zhu, D., Zhang, Y., Li, M., Yao, H.Y., 2011. Postoperative mortality and morbidity in octogenarians and nonagenarians with hip fracture: an analysis of perioperative risk factors. Chin. J. Traumatol. 14, 323–328.

Macchiarelli, R., Bondioli, L., Galichon, V., Tobias, P., 1999. Hip bone trabecular architecture shows uniquely distinctive locomotor behaviour in South African australopithecines. J. Hum. Evol. 36, 211–232.

MacLatchy, L., Muller, R., 2002. A comparison of the femoral head and neck trabecular architecture of Galago and Perodicticus using micro-computed tomography (microCT). J. Hum. Evol. 43, 89–105.

Maga, M., Kappelman, J., Ryan, T.M., Ketcham, R.A., 2006. Preliminary observations on the calcaneal trabecular microarchitecture of extant large-bodied hominoids. Am. J. Phys. Anthropol. 129, 410–417.

Manske, S.L., Liu-Ambrose, T., Cooper, D.M., Kontulainen, S., Guy, P., Forster, B.B., McKay, H.A., 2009. Cortical and trabecular bone in the femoral neck both contribute to proximal femur failure load prediction. Osteoporos. Int. 20, 445–453.

Martin, R.B., Burr, D.B., Sharkey, N.A., 1998. Skeletal Tissue Mechanics. Springer-Verlag, New York.

Mayhew, P.M., Thomas, C.D., Clement, J.G., Loveridge, N., Beck, T.J., Bonfield, W., Burgoyne, C.J., Reeve, J., 2005. Relation between age, femoral neck cortical stability, and hip fracture risk. Lancet 366, 129–135.

Milovanovic, P., Djonic, D., Marshall, R.P., Hahn, M., Nikolic, S., Zivkovic, V., Amling, M., Djuric, M., 2012. Micro-structural basis for particular vulnerability of the superolateral neck trabecular bone in the postmenopausal women with hip fractures. Bone 50, 63–68.

Mitton, D., Rumelhart, C., Hans, D., Meunier, P.J., 1997. The effects of density and test conditions on measured compression and shear strength of cancellous bone from the lumbar vertebrae of ewes. Med. Eng. Phys. 19, 464–474.

Mittra, E., Rubin, C., Qin, Y.X., 2005. Interrelationship of trabecular mechanical and microstructural properties in sheep trabecular bone. J. Biomech. 38, 1229–1237.

Mourtada, F.A., Beck, T.J., Hauser, D.L., Ruff, C.B., Bao, G., 1996. Curved beam model of the proximal femur for estimating stress using dual-energy X-ray absorptiometry derived structural geometry. J. Orthop. Res. 14, 483–492.

Muller, R., Van Campenhout, H., Van Damme, B., Van Der Perre, G., Dequeker, J., Hildebrand, T., Ruegsegger, P., 1998. Morphometric analysis of human bone biopsies: a quantitative structural comparison of histological sections and micro-computed tomography. Bone 23, 59–66.

Nafei, A., Kabel, J., Odgaard, A., Linde, F., Hvid, I., 2000. Properties of growing trabecular ovine bone. Part II. Architectural and mechanical properties. J. Bone Joint Surg. Br. 82, 921–927.

Nagaraja, S., Couse, T.L., Guldberg, R.E., 2005. Trabecular bone microdamage and microstructural stresses under uniaxial compression. J. Biomech. 38, 707–716.

Newman, E., Turner, A.S., Wark, J.D., 1995. The potential of sheep for the study of osteopenia: current status and comparison with other animal models. Bone 16, 277S–284S.

Nyman, J.S., Leng, H., Dong, X.N., Wang, X., 2009. Differences in the mechanical behavior of cortical bone between compression and tension when subjected to progressive loading. J. Mech. Behav. Biomed. 2, 613–619.

Odgaard, A., Dalstra, M., Huiskes, R., Kabal, J., van Rietbergen, B., 1997. Fabric and elastic principal directions of cancellous bone are closely related. J. Biomech. 30, 487–495.

Ohman, J.C., Krochta, T.J., Lovejoy, C.O., Mensforth, R.P., Latimer, B., 1997. Cortical bone distribution in the femoral neck of hominoids: implications for the locomotion of Australopithecus afarensis. Am. J. Phys. Anthropol. 104, 117–131.

Osborne, D., Effmann, E., Broda, K., Harrelson, J., 1980. The development of the upper end of the femur, with special reference to its internal architecture. Radiology 137, 71–76.

Pastoureau, P., Charrier, J., Blanchard, M.M., Biovin, G., Dulor, J.P., Theriez, M., Barenton, B., 1989. Effects of a chronic GFR treatment on lambs having low or normal birth weight. Domest. Anim. Endocrinol. 6, 321–329.

Pidaparti, R.M.V., Turner, C.H., 1997. Cancellous bone architecture: advantages of nonorthogonal trabecular alignment under multidirectional loading. J. Biomech. 30, 979–983.

Pistoia, W., van Rietbergen, B., Ruegsegger, P., 2003. Mechanical consequences of different scenarios for simulated bone atrophy and recovery in the distal radius. Bone 33, 937–945.

Pontzer, H., Lieberman, D.E., Momin, E., Devlin, M.J., Polk, J.D., Hallgrimsson, B., Cooper, D.M., 2006. Trabecular bone in the bird knee responds with high sensitivity to changes in load orientation. J. Exp. Biol. 209, 57–65.

Poole, K.E., Mayhew, P.M., Rose, C.M., Brown, J.K., Bearcroft, P.J., Loveridge, N., Reeve, J., 2010. Changing structure of the femoral neck across the adult female lifespan. J. Bone Miner. Res. 25, 482–491.

Rafferty, K.L., 1998. Structural design of the femoral neck in primates. J. Hum. Evol. 34, 361–383.

Rice, J.C., Cowin, S.C., Bowman, J.A., 1988. On the dependence of the elasticity and strength of cancellous bone on apparent density. J. Biomech. 21, 155–168.

Rincon-Kohli, L., Zysset, P.K., 2009. Multi-axial mechanical properties of human trabecular bone. Biomech. Model. Mechanobiol. 8, 195–208.

Rudman, K.E., Aspden, R.M., Meakin, J.R., 2006. Compression or tension? The stress distribution in the proximal femur. Biomed. Eng. Online 5, 12.

Ruff, C.B., McHenry, H.M., Thackeray, F., Berger, L.R., 1999. Femoral neck cross-sectional morphology in South African early hominids. Am. J. Phys. Anthropol. 28, 237.

Ryan, T.M., Krovitz, G.E., 2006. Trabecular bone ontogeny in the human proximal femur. J. Hum. Evol. 51, 591–602.

Ryan, T.M., Walker, A., 2010. Trabecular bone structure in the humeral and femoral heads of anthropoid primates. Anat. Rec. 293, 719–729.

Sanyal, A., Gupta, A., Bayraktar, H.H., Kwon, R.Y., Keaveny, T.M., 2012. Shear strength behavior of human trabecular bone. In: 58th Annual Meeting of the Orthopaedic Research Society, vol. 37, p. 0125.

Saparin, P., Scherf, H., Hublin, J.J., Fratzl, P., Weinkamer, R., 2011. Structural adaptation of trabecular bone revealed by position resolved analysis of proximal femora of different primates. Anat. Rec. 294, 55–67.

Shaw, C.N., Ryan, T.M., 2012. Does skeletal anatomy reflect adaptation to locomotor patterns? Cortical and trabecular architecture in human and nonhuman anthropoids. Am. J. Phys. Anthropol. 147, 187–200.

Skedros, J.G., Baucom, S.L., 2007. Mathematical analysis of trabecular 'trajectories' in apparent trajectorial structures: the unfortunate historical emphasis on the human proximal femur. J. Theor. Biol. 244, 15–45.

Skedros, J.G., Brand, R.A., 2011. Biographical sketch: Georg Hermann von Meyer (1815–1892). Clin. Orthop. Relat. Res. 469, 3072–3076.

Skedros, J.G., Bloebaum, R.D., Mason, M.W., Bramble, D.M., 1994a. Analysis of a tension/compression skeletal system: possible strain-specific differences in the hierarchical organization of bone. Anat. Rec. 239, 396–404.

Skedros, J.G., Mason, M.W., Bloebaum, R.D., 1994b. Differences in osteonal micromorphology between tensile and compressive cortices of a bending skeletal system: indications of potential strain-specific differences in bone microstructure. Anat. Rec. 239, 405–413.

Skedros, J.G., Su, S.C., Bloebaum, R.D., 1997. Biomechanical implications of mineral content and microstructural variations in cortical bone of horse, elk, and sheep calcanei. Anat. Rec. 249, 297–316.

Skedros, J.G., Mason, M.W., Bloebaum, R.D., 2001. Modeling and remodeling in a developing artiodactyl calcaneus: a model for evaluating Frost's mechanostat hypothesis and its corollaries. Anat. Rec. 263, 167–185.

Skedros, J.G., Hunt, K.J., Bloebaum, R.D., 2004. Relationships of loading history and structural and material characteristics of bone: development of the mule deer calcaneus. J. Morphol. 259, 281–307.

Skedros, J.G., Sorenson, S.M., Hunt, K.J., Holyoak, J.D., 2007. Ontogenetic structural and material variations in ovine calcanei: a model for interpreting bone adaptation. Anat. Rec. 290, 284–300.

Skedros, J.G., Mendenhall, S.D., Kiser, C.J., Winet, H., 2009. Interpreting cortical bone adaptation and load history by quantifying osteon morphotypes in circularly polarized light images. Bone 44, 392–403.

Skedros, J.G., Kiser, C.J., Keenan, K.E., Thomas, S.C., 2011a. Analysis of osteon morphotype scoring schemes for interpreting load history: evaluation in the chimpanzee femur. J. Anat. 218, 480–499.

Skedros, J.G., Sybrowsky, C.L., Anderson, W.E., Chow, F., 2011b. Relationships between in vivo microdamage and the remarkable regional material and strain heterogeneity of cortical bone of adult deer, elk, sheep and horse calcanei. J. Anat. 219, 722–733.

Skedros, J.G., Keenan, K.E., Halley, J.A., Knight, A.N., Bloebaum, R.D., 2012a. Osteon morphotypes and predominant collagen fiber orientation are adaptations for habitual medial-lateral bending in the human proximal diaphysis: implications for understanding the etiology of atypical fractures. In: 58th Annual Meeting of the Orthopaedic Research Society, vol. 37, pp. 1512.

Skedros, J.G., Knight, A.N., Farnsworth, R.W., Bloebaum, R.D., 2012b. Do regional modifications in tissue mineral content and microscopic mineralization heterogeneity adapt trabecular bone tracts for habitual bending? Analysis in the context of trabecular architecture of deer calcanei. J. Anat. 220, 242–255.

Skedros, J.G., Keenan, K.E., Williams, T.J., Kiser, C.J., 2013. Secondary osteon size and collagen/lamellar organization ('osteon morphotypes') are not coupled, but potentially adapt independently for local strain mode or magnitude. J. Struct. Biol. 181, 95–107.

Skerry, T.M., Lanyon, L.E., 1995. Interruption of disuse by short duration walking exercise does not prevent bone loss in the sheep calcaneus. Bone 16, 269–274.

Smith, R.J., Jungers, W.L., 1997. Body mass in comparative primatology. J. Hum. Evol. 32, 523–559.

Srinivasan, B., Kopperdahl, D.L., Amin, S., Atkinson, E.J., Camp, J., Robb, R.A., Riggs, B.L., Orwoll, E.S., Melton 3rd, L.J., Keaveny, T.M., Khosla, S., 2012. Relationship of femoral neck areal bone mineral density to volumetric bone mineral density, bone size, and femoral strength in men and women. Osteoporos. Int. 23, 155–162.

Stauber, M., Muller, R., 2006. Volumetric spatial decomposition of trabecular bone into rods and plates – a new method for local bone morphometry. Bone 38, 475–484.

Stauber, M., Rapillard, L., van Lenthe, G.H., Zysset, P., Muller, R., 2006. Importance of individual rods and plates in the assessment of bone quality and their contribution to bone stiffness. J. Bone Miner. Res. 21, 586–595.

Su, S., 1998. Microstructure and mineral content correlations to strain parameters in cortical bone of the artiodactyl calcaneus. Ph.D. Dissertation. University of Utah.

Su, S.C., Skedros, J.G., Bachus, K.N., Bloebaum, R.D., 1999. Loading conditions and cortical bone construction of an artiodactyl calcaneus. J. Exp. Biol. 202, 3239–3254.

Swartz, S., Parker, A., Huo, C., 1998. Theoretical and empirical scaling patterns and topological homology in bone trabeculae. J. Exp. Biol. 201, 573–590.

Thomas, C.D., Mayhew, P.M., Power, J., Poole, K.E., Loveridge, N., Clement, J.G., Burgoyne, C.J., Reeve, J., 2009. Femoral neck trabecular bone: loss with aging and role in preventing fracture. J. Bone Miner. Res. 24, 1808–1818.

Turner, A.S., 2002. The sheep as a model for osteoporosis in humans. Vet. J. 163, 232–239.

Ulrich, D., van Rietbergen, B., Laib, A., Ruegsegger, P., 1999. The ability of three-dimensional structural indices to reflect mechanical aspects of trabecular bone. Bone 25, 55–60.

van der Meulen, M.C., Morgan, T.G., Yang, X., Baldini, T.H., Myers, E.R., Wright, T.M., Bostrom, M.P., 2006. Cancellous bone adaptation to in vivo loading in a rabbit model. Bone 38, 871–877.

van der Meulen, M.C., Yang, X., Morgan, T.G., Bostrom, M.P., 2009. The effects of loading on cancellous bone in the rabbit. Clin. Orthop. Relat. Res. 467, 2000–2006.

Viola, T., 2002. Locomotion dependent variation in the proximal femoral trabecular pattern in primates. M.Sc. Thesis. University of Vienna.

Wang, Y., Liu, G., Li, T., Xiao, Y., Han, Q., Xu, R., Li, Y., 2010. Morphometric comparison of the lumbar cancellous bone of sheep, deer, and humans. Comp. Med. 60, 374–379.

Wang, J., Zhou, B., Shi, X.T., Liu, X.S., Guo, X.E., 2012. Bone mineral density (BMD) of individual trabecula in human trabecular bone. In: 58th Annual Meeting of the Orthopaedic Research Society, vol. 37, p. 0134.

Whitehouse, W.J., Dyson, E.D., 1974. Scanning electron microscope studies of trabecular bone in the proximal end of the human femur. J. Anat. 118, 417–444.

Wolfram, U., Wilke, H.J., Zysset, P.K., 2011. Damage accumulation in vertebral trabecular bone depends on loading mode and direction. J. Biomech. 44, 1164–1169.

Wu, Z., Niebur, G.L., 2012. Microdamage in human femoral trabecular bone depends on loading mode and pre-existing damage. In: 58th Annual Meeting of the Orthopaedic Research Society, vol. 37, p. 1372.

Young, W.C., 1989. Roark's Formulas for Stress and Strain, sixth ed. McGraw-Hill, New York.

Zarrinkalam, M.R., Beard, H., Schultz, C.G., Moore, R.J., 2009. Validation of the sheep as a large animal model for the study of vertebral osteoporosis. Eur. Spine J. 18, 244–253.

Zebaze, R.M., Jones, A., Welsh, F., Knackstedt, M., Seeman, E., 2005. Femoral neck shape and the spatial distribution of its mineral mass varies with its size: clinical and biomechanical implications. Bone 37, 243–252.